

## Second-harmonic generation in the system with fractional diffraction

Pengfei Li<sup>a,\*</sup>, Hidetsugu Sakaguchi<sup>b</sup>, Liangwei Zeng<sup>c</sup>, Xing Zhu<sup>c</sup>, Dumitru Mihalache<sup>d</sup>, Boris A. Malomed<sup>e,f</sup>

<sup>a</sup>*Department of Physics, Taiyuan Normal University, Jinzhong, 030619, China*

<sup>b</sup>*Interdisciplinary Graduate School of Engineering Sciences, Kyushu University, Kasuga, Fukuoka 816-8580, Japan*

<sup>c</sup>*Department of Basic Course, Guangzhou Maritime University, Guangzhou 510725, China*

<sup>d</sup>*Horia Hulubei National Institute of Physics and Nuclear Engineering, Magurele, Bucharest, RO-077125, Romania*

<sup>e</sup>*Department of Physical Electronics, School of Electrical Engineering, Faculty of Engineering, and Center for Light-Matter Interaction, Tel Aviv University, Tel Aviv 69978, Israel*

<sup>f</sup>*Instituto de Alta Investigación, Universidad de Tarapacá, Casilla 7D, Arica, Chile*

---

### Abstract

We construct a family of bright optical solitons composed of fundamental-frequency (FF) and second-harmonic (SH) components in the one-dimensional (planar) waveguide with the quadratic (second-harmonic-generating) nonlinearity and effective fractional diffraction, characterized by the Lévy index  $\alpha$ , taking values between 2 and 0.5, which correspond to the non-fractional diffraction and critical collapse, respectively. The existence domain and stability boundary for the solitons are delineated in the space of  $\alpha$ , FF-SH mismatch parameter, and propagation constant. The stability boundary is tantamount to that predicted by the Vakhitov-Kolokolov criterion, while unstable solitons spontaneously evolve into localized breathers. A sufficiently weak transverse kick applied to the stable solitons excite small internal vibrations in the stable solitons, without setting them in motion. A stronger kick makes the solitons' trajectories tilted, simultaneously destabilizing the solitons.

---

\*Corresponding author  
*Email address:* `lipf@tynu.edu.cn` (Pengfei Li<sup>a,\*</sup>)

**Keywords:** Second-harmonic generation; Fractional diffraction; Lévy index; Quadratic nonlinearity; Bright solitons; Soliton stability; Breathers

---

## 1. Introduction

The concept of the fractional spatial dispersion has been first brought to the forefront of research in physics in the framework of fractional quantum mechanics for particles moving by Lévy flights [1, 2, 3, 4]. Particular implementations of the fractional Schrödinger equations were proposed in Lévy crystals [5] and polariton condensates [6], although experimental realization of the fractional quantum mechanics has not been reported, as yet. On the other hand, it was proposed to make use of the commonly known similarity of the Schrödinger equation and the classical equation for the paraxial light propagation, and implement the fractional diffraction in optics, which will emulate the action of the fractional kinetic-energy operator in the quantum theory [7]. The proposal relied on using the  $4f$  optical setup to split the light beam into spectral components corresponding to different values of the transverse wave number by means of a lens, passing the separated components through an appropriately designed phase plate, which should impart to them phase shifts emulating the action of the fractional diffraction, and recombining the components back into a single beam by means of the second lens.

In the optical system, it is natural to combine the fractional diffraction with the nonlinearity of optical materials, which leads to the introduction of various forms of the fractional nonlinear Schrödinger (NLS) equations and prediction of a variety of fractional solitons and nonlinear phenomena, such as accessible [8, 9], gap [10, 11, 12], and surface [13, 14] solitons, solitary vortices [15], fractional solitons in nonlinear lattice [16], wave collapse [17], and other nonlinear effects [18]-[27]. Another natural extension was developed for optical waveguides and cavities combining fractional diffraction with losses, gain, and nonlinearity, leading to models in the form of fractional NLS equations with  $\mathcal{PT}$ -symmetric complex potentials, that also give rise to a variety of soliton states [28]-[35].

Further, solitons [36]-[38] and domain-wall states [39] were predicted as solutions of systems of coupled fractional NLS equations. A part of these findings were summarized in Ref. [40].

An important branch of nonlinear optics, including the formation of solitons, is based on the second-harmonic generation in media with quadratic ( $\chi^{(2)}$ ) nonlinearity [41]-[53]. In this work, we systematically investigate the formation and stability of bright solitons in the system with the fractional diffraction acting on both the fundamental-frequency (FF) and second-harmonic (SH) waves coupled by the  $\chi^{(2)}$  interaction.

The rest of the paper is organized as follows. The model is introduced in Section 2. It includes the considerations of the cascading limit, which replaces the quadratic nonlinearity by an effective cubic one. Systematic results for families of stationary solitons and their stability are reported in Section 3. Dynamics of the solitons is addressed in Section 4. The paper is concluded by Section 5.

## 2. The model

### 2.1. The fractional system with the $\chi^{(2)}$ interaction

The starting point is the system of one-dimensional coupled nonlinear equations for amplitudes of the FF and SH waves,  $\Psi_1(x, z)$  and  $\Psi_2(x, z)$ :

$$i\frac{\partial\Psi_1}{\partial z} - D_1\left(-\frac{\partial^2}{\partial x^2}\right)^{\alpha/2}\Psi_1 + \Psi_1^*\Psi_2 = 0, \quad (1)$$

$$2i\frac{\partial\Psi_2}{\partial z} - D_2\left(-\frac{\partial^2}{\partial x^2}\right)^{\alpha/2}\Psi_2 + Q\Psi_2 + \frac{1}{2}\Psi_1^2 = 0, \quad (2)$$

where  $z$  is the propagation distance,  $x$  is the transverse coordinate, while  $D_1$  and  $D_2$  are the FF and SH diffraction coefficients. Real  $Q$  is the mismatch parameter of the  $\chi^{(2)}$  interaction, with  $*$  standing for the complex conjugate. The fractional diffraction is represented by Riesz derivative with Lévy index (LI)  $\alpha$  [54, 55],

$$\left(-\frac{\partial^2}{\partial x^2}\right)^{\alpha/2}\Psi(x) = \frac{1}{2\pi}\int_{-\infty}^{+\infty}|p|^\alpha dp \int_{-\infty}^{+\infty}d\xi e^{ip(x-\xi)}\Psi(\xi). \quad (3)$$

Normally, LI takes values  $1 < \alpha \leq 2$ , but it is also possible to consider values  $0 < \alpha \leq 1$ . The usual diffraction corresponds to  $\alpha = 2$ . Straightforward analysis demonstrates that Eqs. (1) and (2) with the quadratic nonlinearity do not produce the collapse in the interval of

$$1/2 < \alpha \leq 2. \quad (4)$$

The critical and supercritical collapse occurs at  $\alpha = 1/2$  and  $\alpha < 1/2$ , respectively (recall that the combination of the fractional diffraction with the cubic nonlinearity gives rise to the collapse at  $\alpha \leq 1$  [40]).

Stationary solutions to Eqs. (1) and (2) with FF and SH propagation constants  $\beta_1$  and  $\beta_2 \equiv 2\beta_1$  are looked for as

$$\Psi_1(x, z) = e^{i\beta_1 z} \psi_1(x), \quad \Psi_2(x, z) = e^{2i\beta_1 z} \psi_2(x), \quad (5)$$

where the real functions  $\psi_{1,2}(x)$  satisfy the following system of stationary equations:

$$-D_1 \left( -\frac{\partial^2}{\partial x^2} \right)^{\alpha/2} \psi_1 - \beta_1 \psi_1 + \psi_1^* \psi_2 = 0, \quad (6)$$

$$-D_2 \left( -\frac{\partial^2}{\partial x^2} \right)^{\alpha/2} \psi_2 + Q\psi_2 - 4\beta_1 \psi_2 + \frac{1}{2} \psi_1^2 = 0. \quad (7)$$

Two-wave soliton families may be naturally characterized, as usual, by dependences between the propagation constant  $\beta_1$  and the power (alias the Manley-Rowe invariant, or the soliton's norm),

$$N = \int_{-\infty}^{+\infty} \left( |\psi_1|^2 + 4|\psi_2|^2 \right) dx, \quad (8)$$

which is a dynamical invariant of the underlying system of Eqs. (1) and (2).

## 2.2. The cascading limit for $Q < 0$ and the scaling invariance for $Q = 0$

The approximation known as the cascading limit (CL) corresponds, roughly speaking, to large values of  $|Q|$ . In this case, one neglects the fractional-derivative and propagation-constant terms in comparison with other linear terms in Eq. (7), which yields

$$\psi_2 \approx - (2Q)^{-1} \psi_1^2. \quad (9)$$

The substitution of approximation (9) in Eq. (6) yields a single fractional equation with the cubic nonlinearity:

$$-D_1 \left( -\frac{\partial^2}{\partial x^2} \right)^{\alpha/2} \psi_1 - \beta_1 \psi_1 - \frac{1}{2Q} |\psi_1|^2 \psi_1 = 0. \quad (10)$$

Obviously, Eq. (10) with  $\alpha \geq 1$  and  $Q < 0$  has solitons solutions, without any threshold (critical) value  $N_{\text{cr}}$  of the norm (8) necessary for the existence of the solitons [i.e.,  $N_{\text{cr}}(Q < 0, \alpha \geq 1) = 0$ ]. On the contrary, Eq. (10) with  $Q > 0$  has no bright-soliton solutions for any value of LI  $\alpha$ . At  $Q < 0$  and  $\alpha < 1$ , the situation is more complex, because the  $z$ -dependent version of Eq. (10) gives rise to the supercritical collapse in that case.

It is relevant to note that, for  $\beta_1 \rightarrow +0$ , it follows from Eqs. (10) and (9) that the width  $L$  and amplitudes  $A_{1,2} \equiv (|\psi_{1,2}(x)|)_{\text{max}}$  of the corresponding broad solitons asymptotically scale as

$$L \sim \beta_1^{-1/\alpha}, A_1 \sim \sqrt{\beta_1}, A_2 \sim \beta_1, \quad (11)$$

hence the power (8) scales as

$$N \sim \beta_1^{1-1/\alpha}. \quad (12)$$

Numerical results for the system with  $Q = -1$ , presented below in Figs. 1(a) and 2(a), corroborate the asymptotic relation (12) for  $\alpha > 1$ , while for  $\alpha < 1$  the numerical solution of the full system of equations (6) and (7) demonstrates that the solitons exist only above a finite threshold (critical) value of the norm,  $N > N_{\text{cr}}$ , hence CL does not apply to the case of  $\alpha < 1$ .

In the case of  $Q = 0$ , when the CL is not relevant, Eqs. (1) and (2) admit *exact* scaling invariance (not restricted to  $\beta_1 \rightarrow 0$ ). The exact relation between  $L$  and  $\beta_1 \rightarrow 0$  is the same as its asymptotic counterpart in Eq. (11), while the exact scalings of the amplitude and power are different:

$$(A_{1,2}(Q = 0))_{\text{exact}} \sim \beta_1, (N(Q = 0))_{\text{exact}} \sim \beta_1^{2-1/\alpha}. \quad (13)$$

Further, it is worthy to note that, in interval (4), relation  $N(\beta_1)$  in Eq. (13) satisfies the well-known necessary stability condition given by the Vakhitov-Kolokolov (VK) criterion,  $dN/d\beta_1 > 0$  [56, 57]. On the other hand, precisely

at  $\alpha = 1/2$ , Eq. (13) yields  $dN/d\beta_1 = 0$ , which is a signature of the above-mentioned critical collapse [57].

Below, scaling is used to set  $Q = \pm 1$ , unless  $Q = 0$  (the scaling does not imply that CL is not relevant). Taking this definition into regard, we conclude that the predictions of CL agree, in particular, with numerical results displayed in Fig. 3, which shows  $N_{\text{cr}} = 0$  for  $Q = -1$  and  $\alpha \geq 1$ , and  $N_{\text{cr}} > 0$  in the case of  $Q = +1$ , in accordance with the fact that CL predicts no solitons with  $N \rightarrow 0$  in the latter case.

### 3. Stationary modes

#### 3.1. The existence range of solitons

Numerical solutions of Eqs. (6) and (7) for stationary two-component solitons, with the FF and SH propagation constants  $\beta_1$  and  $\beta_2 \equiv 2\beta_1$ , were produced by means of the Newton-conjugate-gradient method [58]. The results are presented separately for different values of the mismatch parameter normalized as mentioned above, i.e.,  $Q = 0$  and  $\pm 1$ . By means of rescaling of coordinate  $x$ , we set  $D_1 = 1/2$ . Further, because the diffraction has a universal form for all wave components, we also set  $D_2 = 1/2$ .

The solutions were constructed in interval (4) in which, as mentioned above, the system is free of collapsing. Soliton families are characterized by dependences  $N(\beta_1)$  for power (8), which are displayed for three characteristic LI values,  $\alpha = 1.5, 1.0$ , and  $0.7$ , and for the negative, zero, and positive mismatch,  $Q = -1, 0$ , and  $1$ , in Figs. 1(a,b,c).

First, we note that, as predicted above by CL in the case of  $Q = -1$  and  $\alpha > 1$ , the solitons exist in Fig. 1(a) (actually, for  $\alpha = 1.5$ ) for all values of  $N > 0$ , i.e., there is no threshold value of the norm necessary for their existence. Also in agreement with CL, this soliton family satisfies the VK criterion,  $d\beta_1/dN > 0$  (and it is indeed a completely stable family). Furthermore, the segment of the  $\beta_1(N; \alpha = 1.5)$  curve at  $\beta_1 \rightarrow 0$  is consistent with the asymptotic relation (11), which predicts, in this case,  $\beta_1 \sim N^3$  (precise comparison with the latter

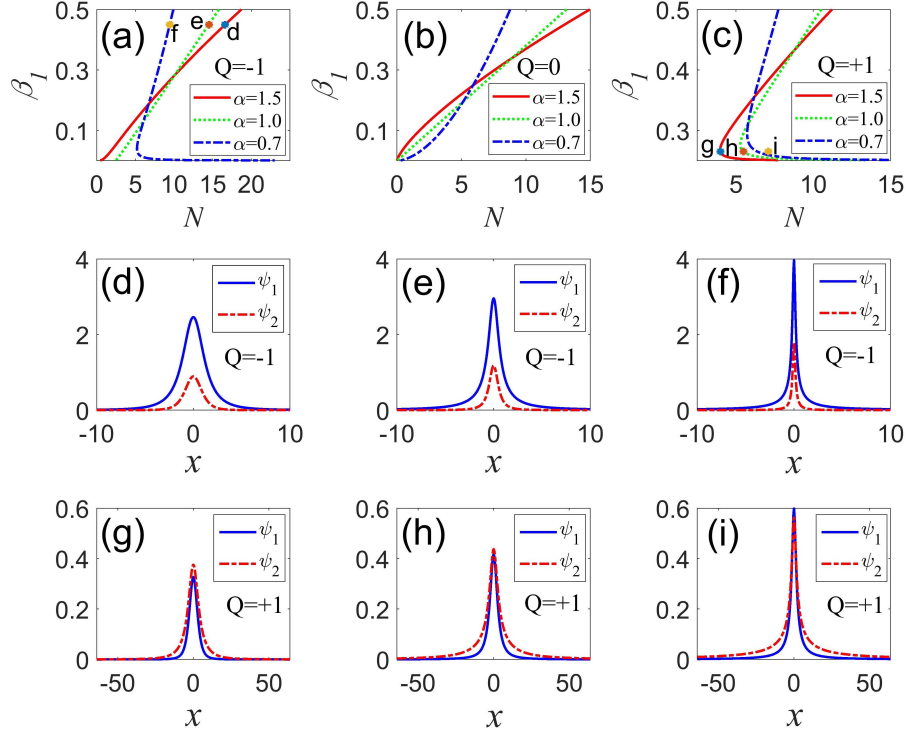


Figure 1: The FF propagation constant of the bright solitons,  $\beta_1$ , vs. the total power,  $N$ , for LI values  $\alpha = 1.5, 1.0$  and  $0.7$ , as produced by the numerical solutions of Eqs. (6) and (7). Panels (a), (b), and (c) display the  $\beta_1(N)$  curves for values of the mismatch parameter  $Q = -1, 0$ , and  $+1$ , respectively, and for the different values of LI, as indicated in the figures. The respective soliton families are stable when they satisfy the the VK criterion,  $d\beta_1/dN > 0$ . Panels (d), (e), and (f) display examples of stable bright solitons with the FF and SH components  $\psi_1(x)$  and  $\psi_2(x)$  (blue solid and red dashed-dotted lines, respectively), for a fixed value of  $\beta_1 = 0.45$  and mismatch  $Q = -1$ . They correspond to points marked by stars and the same labels, d, e, and f, in panel (a), which identify the respective values of LI. Panels (g), (h), and (i) display examples of bright solitons for a fixed value of  $\beta_1 = 0.265$  and mismatch  $Q = +1$ . They correspond to points marked by stars and the same labels, g, h, and i, in panel (c), which identify the respective values of LI.

prediction is difficult, as one should use an extremely broad integration domain to produce accurate results for very broad solitons in the limit of  $\beta_1 \rightarrow 0$ ).

For  $\alpha = 1.5$  and  $1.0$ , the propagation constant  $\beta_1$  is a monotonously growing function of the power in Fig. 1(a) for  $Q = -1$ , while the curve for  $\alpha = 0.7$  is divided in two branches, with positive and negative slopes,  $d\beta_1/dN > 0$  and  $d\beta_1/dN < 0$ , indicating that the bright solitons exist at  $N > N_{\text{cr}}$ . Only the branch with  $d\beta_1/dN > 0$  may be stable, according to the VK criterion.

Further, the  $\beta_1(N)$  dependences shown for  $Q = 0$  in Fig. 1(b) fully corroborate the exact relation (13). For example, for  $\alpha = 1$  the dependence is precisely linear, as predicted by Eq. (13), *viz.*,  $\beta_1 = 0.038N$ , where the proportionality coefficient is extracted from the numerical data.

Next, Fig. 1(c) shows that all  $\beta_1(N)$  curves for  $Q = +1$  are divided into branches with positive and negative slopes, demonstrating the existence of a finite threshold (critical) value,  $N_{\text{cr}} > 0$ . All the turning points in Fig. 1(c), with  $N = N_{\text{cr}}$ , correspond to very close values of the propagation constant,  $\beta_1 \simeq 0.27$ . This value can be readily explained by noting that the full coefficient  $(Q - 4\beta_1)$  in front of the linear term in Eq. (7) becomes negative at  $\beta_1 > Q/4 \equiv 0.25$  (recall  $Q = 1$  is fixed in this case) and, accordingly, Eq. (10) with  $Q$  replaced by the full coefficient,  $(Q - 4\beta_1)$ , suggests that solitons may exist at  $\beta_1 > (\beta_1)_{\text{cr}} \approx 0.25$ , even if CL does not exactly apply for relatively small values of  $|Q - 4\beta_1|$ .

Figures 1(d,e,f) show soliton shapes for components  $\psi_1$  and  $\psi_2$  at  $Q = -1$  with a fixed propagation constant,  $\beta_1 = 0.45$ , for the same values of LI as in Fig. 1(a). The amplitudes of  $\psi_1$  and  $\psi_2$  increase, while the widths of the profiles shrink, as the value of LI decreases, as smaller LI makes the diffraction weaker, hence the soliton needs to be narrower, to keep the balance with the nonlinearity. Note that the amplitude and width of the  $\psi_2$  component are essentially smaller than in the  $\psi_1$  components, which is a natural “remnant” of CL, see Eq. (9), even if CL does not directly apply for relatively large values of  $\beta_1$ . Similarly, Figs. 1(g), 1(h) and 1(i) show the solitons at  $Q = +1$  with fixed  $\beta_1 = 0.265$  (close to  $N = N_{\text{cr}}$ ) for the same values of LI as in Fig. 1(c), where the shapes of components  $\psi_1$  and  $\psi_2$  are close, unlike the case of  $Q = -1$ .



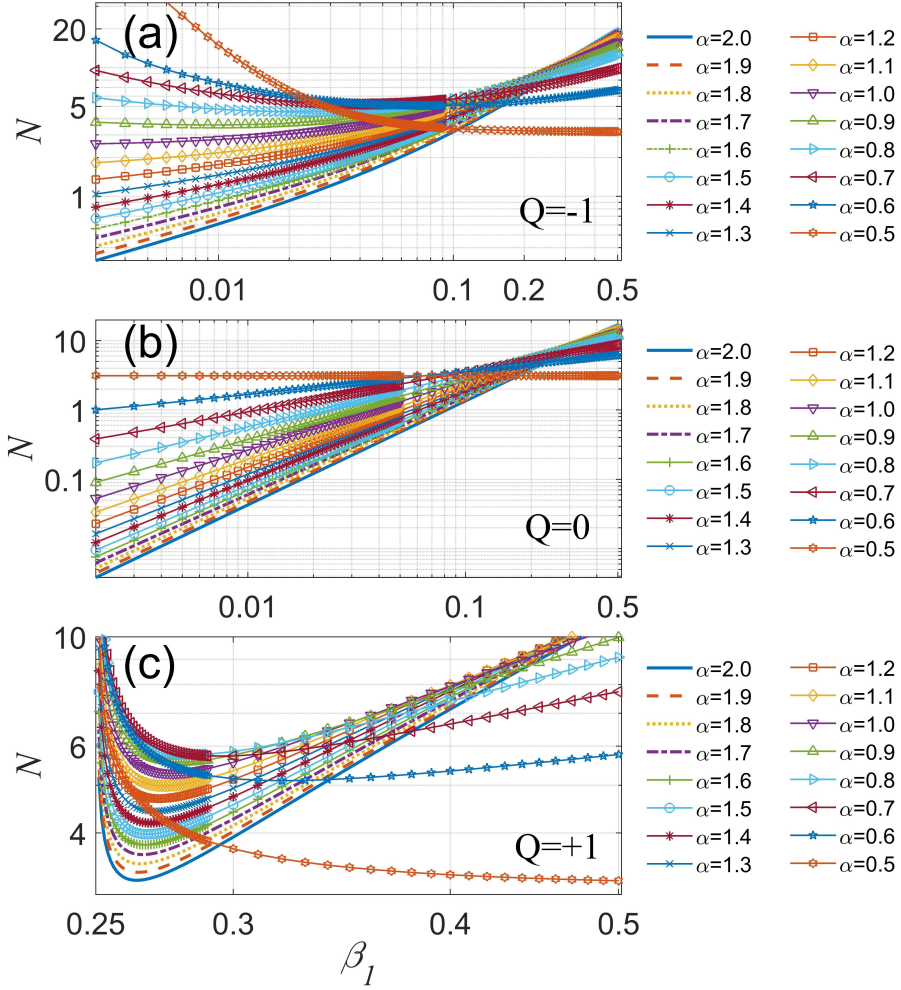


Figure 2: Power curves  $N(\beta_1)$  for soliton families with different values of LI  $\alpha$  and different mismatch parameters: (a)  $Q = -1$ , (b)  $Q = 0$ , and (c)  $Q = +1$ . Note that the logarithmic scales are used for  $N$  and  $\beta_1$  in panels (a) and (b), while (c) is plotted using ordinary scales.

### 3.2. Stability of the solitons

As mentioned above, the necessary stability condition for the families of stationary solitons is given by the VK criterion,  $d\beta_1/dN > 0$ . To summarize these results, a large number of  $N(\beta_1)$  curves are collected, for  $Q = -1, 0$ , and  $+1$ , in Figs. 2(a), (b), and (c), respectively. Each panel includes 16 curves for values of LI covering the interval (4). The range of values of the propagation constant is  $0.002 \leq \beta_1 \leq 0.5$  in Figs. 2(a) and 2(b) for  $Q = -1$  and  $0$ , and is  $0.0251 \leq \beta_1 \leq 0.5$  for  $Q = 1$  in Figs. 2(c). The size of the computation domain is  $X = 16384$  for  $0.7 \leq \alpha \leq 2.0$ ,  $X = 131072$  for  $\alpha = 0.6$ , and  $X = 409600$  for  $\alpha = 0.5$  in Figs. 2(a) and 2(b). Further, it is  $X = 16384$  for  $0.9 \leq \alpha \leq 2.0$  and  $X = 20480$  for  $0.5 \leq \alpha \leq 0.8$  in Fig. 2(c). For very small values of the propagation constant  $\beta_1$ , the results may be affected by the fact that the characteristic width of the solitons, estimated as  $\sim \beta_1^{-1/\alpha}$ , becomes comparable to the size of the integration domain.

As an extension of the trend observed above in Fig. 1(a), all the  $N(\beta_1)$  curves in Fig. 2(a) for  $Q = -1$  show the monotonous growth in the range of  $1 < \alpha \leq 2$ , hence they all meet the VK criterion. Also in agreement with that trend, at  $0.5 < \alpha \leq 1$ , there is a finite critical (threshold) value  $N_{\text{cr}}$ , which divides the power curves in VK-stable and unstable branches, with  $dN/d\beta_1 > 0$  and  $dN/d\beta_1 < 0$ , respectively. In particular, in the limit of  $\alpha = 0.5$ , the dependence  $N(\beta_1)$  is monotonously decreasing, hence all the solitons are unstable in this limit, being subject to the onset of the critical collapse, as indicated by the asymptotically flat dependence for relatively large values of  $\beta_1$ .

The trend suggested above by Fig. 1(b) for  $Q = 0$  is confirmed in detail by Fig. 2(b): all the corresponding  $N(\beta_1)$  curves are monotonously growing at all values of  $\beta_1$  (clearly suggesting  $N_{\text{cr}} = 0$ ) in the entire interval (4), in accordance with Eq. (13), thus providing the VK stability of all solitons in this interval. In the limit case of  $\alpha = 0.5$ , the  $N(\beta_1)$  dependence becomes flat, also in agreement with Eq. (13).

The detailed results for  $Q = +1$  are collected in Fig. 2(c). In this case, all curves, except for the one for  $\alpha = 0.5$ , are divided in VK-stable and un-

stable branches, separated by  $N = N_{\text{cr}}$ . In the limit case of  $\alpha = 0.5$ , the entire  $N(\beta_1)$  curve features a negative slope, i.e., the instability. Note that the unstable branch, with  $dN/d\beta_1 < 0$ , persists in the opposite limit of  $\alpha = 2$ , which corresponds to the usual  $\chi^{(2)}$  system with non-fractional diffraction. It is easy to check that, in this limit, the unstable branch precisely coincides with the previously known one discovered by the analysis of the usual  $\chi^{(2)}$  system [42, 50].

On the contrary to the cases of  $Q = -1$  and  $0$ , where very broad solitons exist with arbitrarily small values of the propagation constant  $\beta_1$  [see Eq. (11)] in the case of  $Q = +1$  the values are limited, according to the form of the linear terms in Eq. (7), to  $\beta_1 > 1/4$  (as was mentioned above). As well as in the limit of  $\beta_1 \rightarrow 0$  for  $Q = -1$  and  $0$ , the limit of  $\beta_1 - 1/4 \rightarrow 0$  for  $Q = +1$  naturally corresponds to solitons with diverging width  $\sim (\beta_1 - 1/4)^{-1/\alpha}$ .

The numerically found dependence of the critical (threshold) power  $N_{\text{cr}}$  on LI in the range of  $0.5 < \alpha \leq 2$  is displayed, for mismatch  $Q = -1$  and  $+1$ , in Figs. 3(a) and (c). As mentioned above, the solitons exist at  $N > N_{\text{cr}}$ , there being no stationary soliton solutions at  $N < N_{\text{cr}}$ . The related dependence of the critical propagation constant  $\beta_{1\text{cr}} \equiv \beta_1(N_{\text{cr}})$  on LI, are boundaries between stable solitons at  $\beta_1 > \beta_{1\text{cr}}$  and unstable ones at  $\beta_1 < \beta_{1\text{cr}}$  for given  $\alpha$ , as shown in Figs. 3(b) and (d). These figures corroborate the above-mentioned conclusion, that, for  $Q = -1$ , stable solitons exist for any  $N > 0$  in the range of  $1 < \alpha \leq 2$ , and for  $N > N_{\text{cr}} > 0$  in the range of  $0.5 < \alpha \leq 1$ ; for  $Q = +1$ , the stable solitons exist only above the threshold value, at  $N > N_{\text{cr}}$ , in the entire interval (4). On the other hand, for  $Q = 0$  all the solitons are stable, as inferred above, for any  $N > 0$  and for all values of LI in interval (4). Lastly, all the solitons are unstable at  $\alpha = 0.5$ , for  $Q = \pm 1$  and  $0$ .

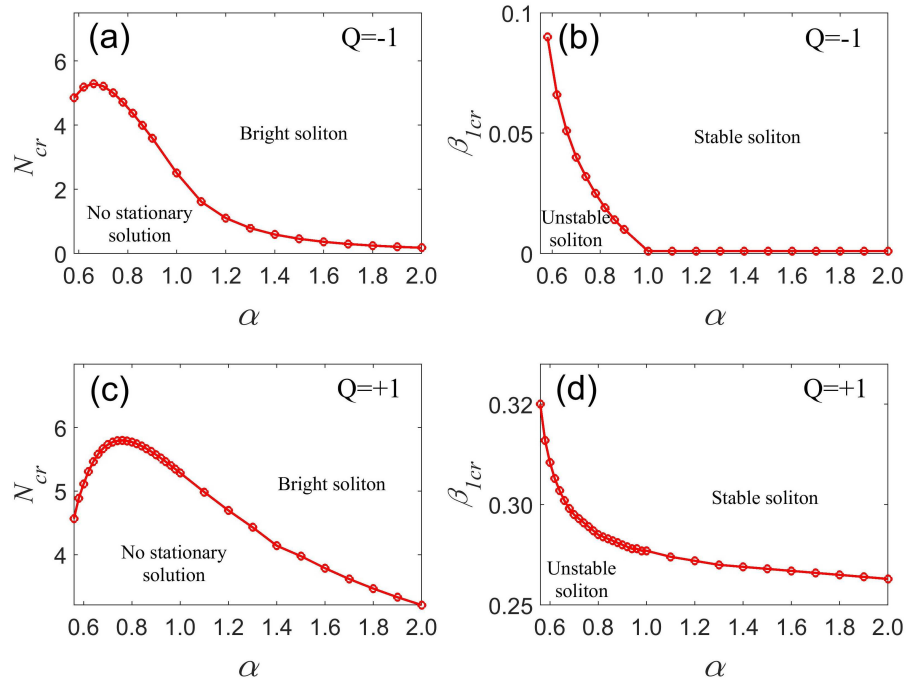


Figure 3: Domains of the existence, stability, and instability of the solitons, divided by the power threshold (critical value)  $N_{cr}$  (a,c) and the respective critical value  $\beta_{1cr}$  of the propagation constant (b,d) for mismatch parameters  $Q = -1$  (a,b) and  $Q = +1$  (c,d).

## 4. Verification of the soliton's stability and instability

### 4.1. Perturbed solutions

Predictions for the (in)stability of the solitons, produced above on the basis of the VK criterion, which, strictly speaking, is a necessary one but not sufficient, were corroborated by the analysis of linearized equations for small perturbations and direct simulations of the perturbed evolution. First, weakly perturbed solutions were looked as

$$\begin{aligned}\Psi_1 &= e^{i\beta_1 z} \left[ \psi_1(x) + u_1(x) e^{\delta z} + u_2^*(x) e^{\delta^* z} \right], \\ \Psi_2 &= e^{i\beta_2 z} \left[ \psi_2(x) + v_1(x) e^{\delta z} + v_2^*(x) e^{\delta^* z} \right],\end{aligned}\quad (14)$$

where  $\psi_{1,2}$  represents the unperturbed soliton, defined as per Eq. (5), while  $u_{1,2}$  and  $v_{1,2}$  are the small perturbations with the respective complex eigenvalue  $\delta$ . The substitution of expression (14) in Eqs. (1) and (2) and linearization leads to the system of coupled equations,

$$\begin{aligned}\delta u_1 &= i \left\{ \left[ -\beta_1 - D_1 \left( -\frac{\partial^2}{\partial x^2} \right)^{\alpha/2} \right] u_1 + v u_2 + u^* v_1 \right\}, \\ \delta u_2 &= i \left\{ -v u_1 + \left[ \beta_1 + D_1 \left( -\frac{\partial^2}{\partial x^2} \right)^{\alpha/2} \right] u_2 - u v_2 \right\}, \\ \delta v_1 &= i \left\{ \frac{1}{2} u u_1 - \left[ \beta_2 + \frac{D_2}{2} \left( -\frac{\partial^2}{\partial x^2} \right)^{\alpha/2} - \frac{Q}{2} \right] v_1 \right\}, \\ \delta v_2 &= i \left\{ -\frac{1}{2} u^* u_2 + \left[ \beta_2 + \frac{D_2}{2} \left( -\frac{\partial^2}{\partial x^2} \right)^{\alpha/2} - \frac{Q}{2} \right] v_2 \right\}.\end{aligned}\quad (15)$$

Equations (15) were solved by means of the Fourier collocation method [58]. The solitons are linearly stable if all eigenvalues  $\delta$  are imaginary, whereas they are unstable in the case if  $\text{Re}(\delta) > 0$  exists.

Direct tests of the perturbed stability of the solitons were performed by simulations of Eqs. (1) and (2) with input taken as per Eq. (14) at  $z = 0$ , using the spectral method combined with the Runge-Kutta one.

#### 4.2. Stable and unstable perturbation eigenvalues and direct propagation

We have corroborated the stability of the solitons, as predicted above by the VK criterion, by results of the linear-stability analysis and direct simulations. Examples are demonstrated in Fig. 4 for  $\alpha = 1.5$ ,  $\beta_1 = 0.5$ , and  $Q = \pm 1$  and 0. It is seen in panels (a<sub>1</sub>)–(a<sub>3</sub>) that VK-stable solitons are indeed linearly stable. To simulate the full system of Eqs. (1) and (2), random perturbations at the 5% amplitude level were added at  $z = 0$  to the stationary solitons, as per Eq. (14).

The VK-predicted instability of the solitons has been verified too. Examples are displayed for  $Q = 1$ ,  $\beta_1 = 0.265$  and several different values of LI in Fig. 5. It is worthy to note that unstable solitons are not fully destroyed by perturbations, but spontaneously transform into robust oscillatory states.

The instability of the solitons for  $\alpha = 0.5$  is also corroborated by direct simulations of Eqs. (1) and (2), see examples in Fig. 6 for propagation constant  $\beta_1 = 0.1$  and mismatch parameters  $Q = -1$  and 0 in Figs. 6(a<sub>1</sub>)–(a<sub>3</sub>) and 6(b<sub>1</sub>)–(b<sub>3</sub>), respectively, and for propagation constant  $\beta_1 = 0.265$  with mismatch parameter  $Q = 1$  in Figs. 6(c<sub>1</sub>)–(c<sub>3</sub>). In these examples, the critical collapse manifests itself by sudden decay of both the FF and SH components.

#### 4.3. Kicked solitons

The fractional diffraction breaks the Galilean invariance of underlying equations (1) and (2) [40], therefore attempts to construct solutions for “moving” solitons (actually, for ones tilted in the spatial domain) is a nontrivial objective. It may be addressed by taking a stable stationary soliton and applying transverse kicks  $k$  and  $2k$  to its FF and SH components, i.e., simulating (1) and (2) with input

$$\Psi_1(x) = \psi_1(x) \exp(ikx), \Psi_2(x) = \psi_2(x) \exp(2ikx). \quad (16)$$

The simulations demonstrate that, for  $k$  small enough, the kick *does not* initiate motion, in contrast with the commonly known result for the Galilean-invariant systems, such as Eqs. (1) and (2) with the non-fractional diffraction,  $\alpha = 2$ .

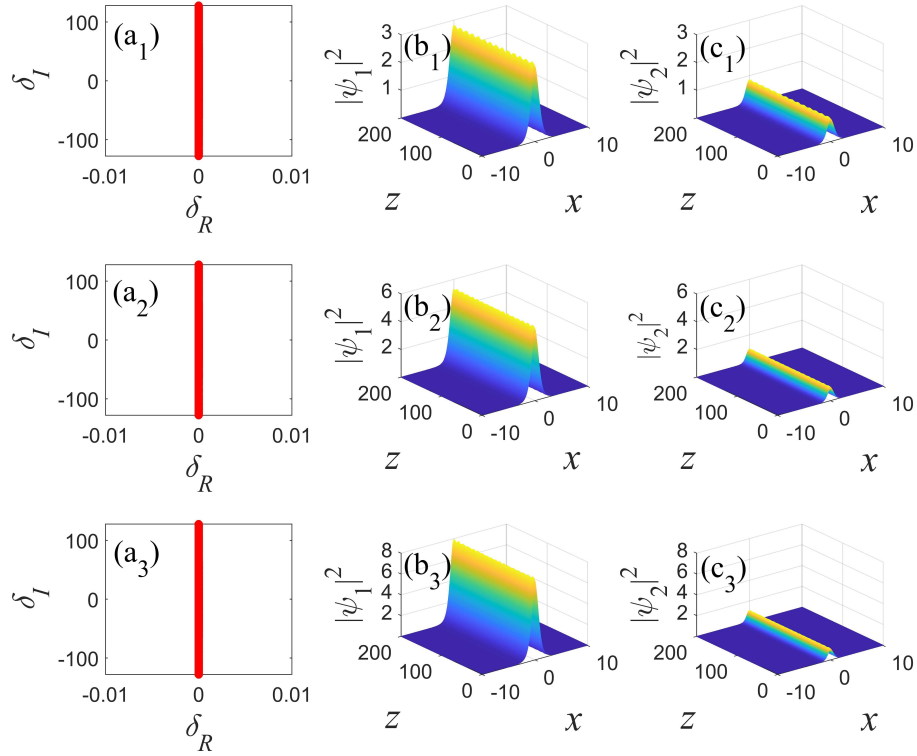


Figure 4: Linear-stability spectra for stable solitons (a<sub>1</sub>, a<sub>2</sub>, a<sub>3</sub>) and the simulated evolution of the FF and SH components initiated with 5% random perturbations (b<sub>1</sub>, b<sub>2</sub>, b<sub>3</sub>) and (c<sub>1</sub>, c<sub>2</sub>, c<sub>3</sub>). Values of the mismatch parameter corresponding to the top, middle, and bottom rows are  $Q = +1, 0$ , and  $-1$ , respectively. Other parameters are fixed as  $\beta_1 = 0.5$  and  $\alpha = 1.5$ .

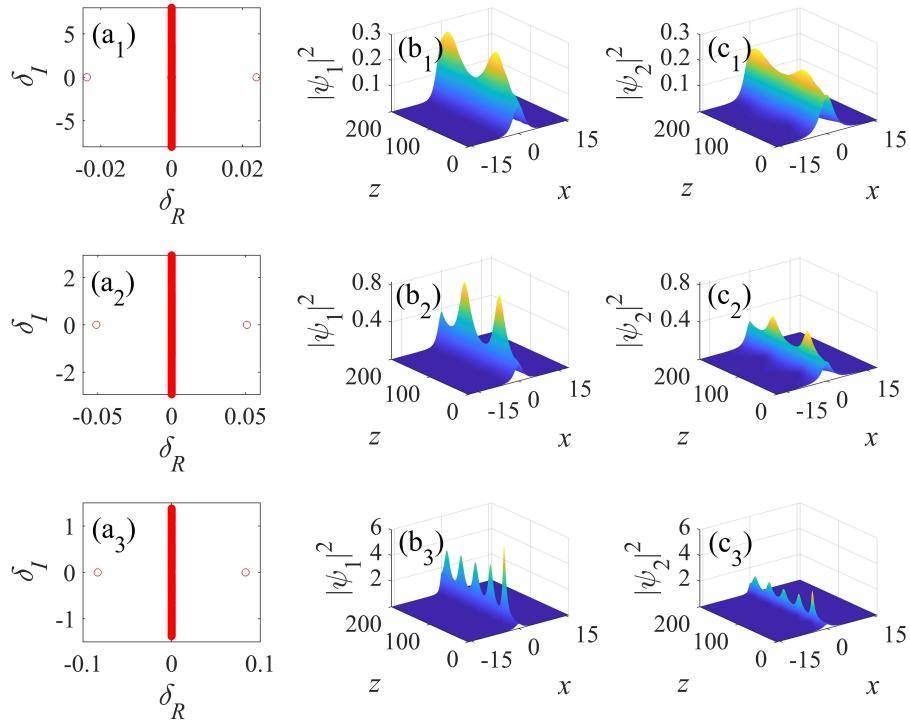


Figure 5: The linear-stability spectra (a<sub>1</sub>,a<sub>2</sub>,a<sub>3</sub>) and perturbed evolution of FF and SH components (b<sub>1</sub>,b<sub>2</sub>,b<sub>3</sub>) and (c<sub>1</sub>,c<sub>2</sub>,c<sub>3</sub>) for VK-unstable solitons with mismatch parameter  $Q = 1$  and propagation constant  $\beta_1 = 0.265$ . Top, middle, and bottom rows correspond, respectively, to different LI values, *viz.*,  $\alpha = 1.5$ ,  $\alpha = 1.0$ , and  $\alpha = 0.7$ .



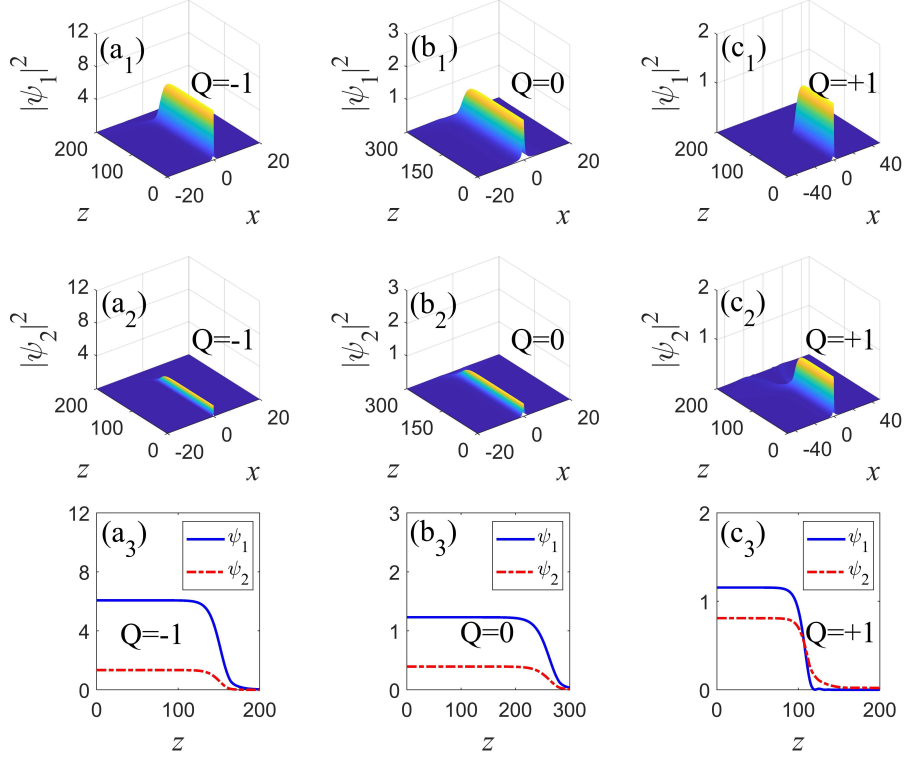


Figure 6: The unstable evolution of the FF and SH components of the solitons at the value of LI  $\alpha = 0.5$ , at which Eqs. (1) and (2) give rise to the critical collapse. Panels (a<sub>1</sub>–a<sub>3</sub>), (b<sub>1</sub>–b<sub>3</sub>) display examples of the spontaneous decay for values of the mismatch  $Q = -1$  and  $0$ , respectively, with fixed propagation constant  $\beta_1 = 0.1$ . Panels (c<sub>1</sub>–c<sub>3</sub>) display the spontaneous decay for the mismatch  $Q = +1$  with fixed propagation constant  $\beta_1 = 0.265$ .

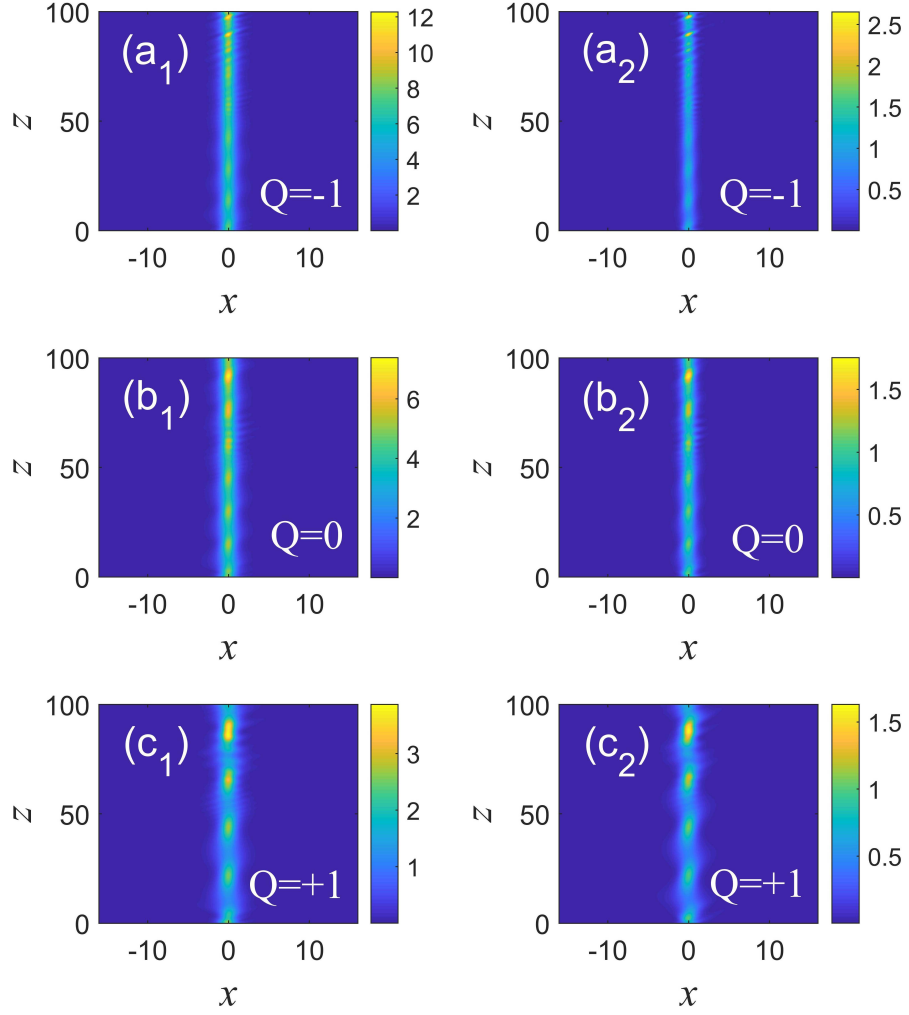


Figure 7: The evolution of a soliton initiated by kick  $k = 0.3$  in Eq. (16), displayed by means of local-density maps of the FF and SH local powers,  $|\psi_1(x,z)|^2$  and  $|\psi_2(x,z)|^2$ , in the left and right panels, respectively. The top, middle, and bottom rows of panels correspond to the mismatch parameters  $Q = -1, 0,$  and  $+1$ , respectively. Other parameters are  $\beta_1 = 0.5$  and  $\alpha = 1.5$ . In this case, the kick excites an intrinsic mode in the soliton, but does not set it in motion.

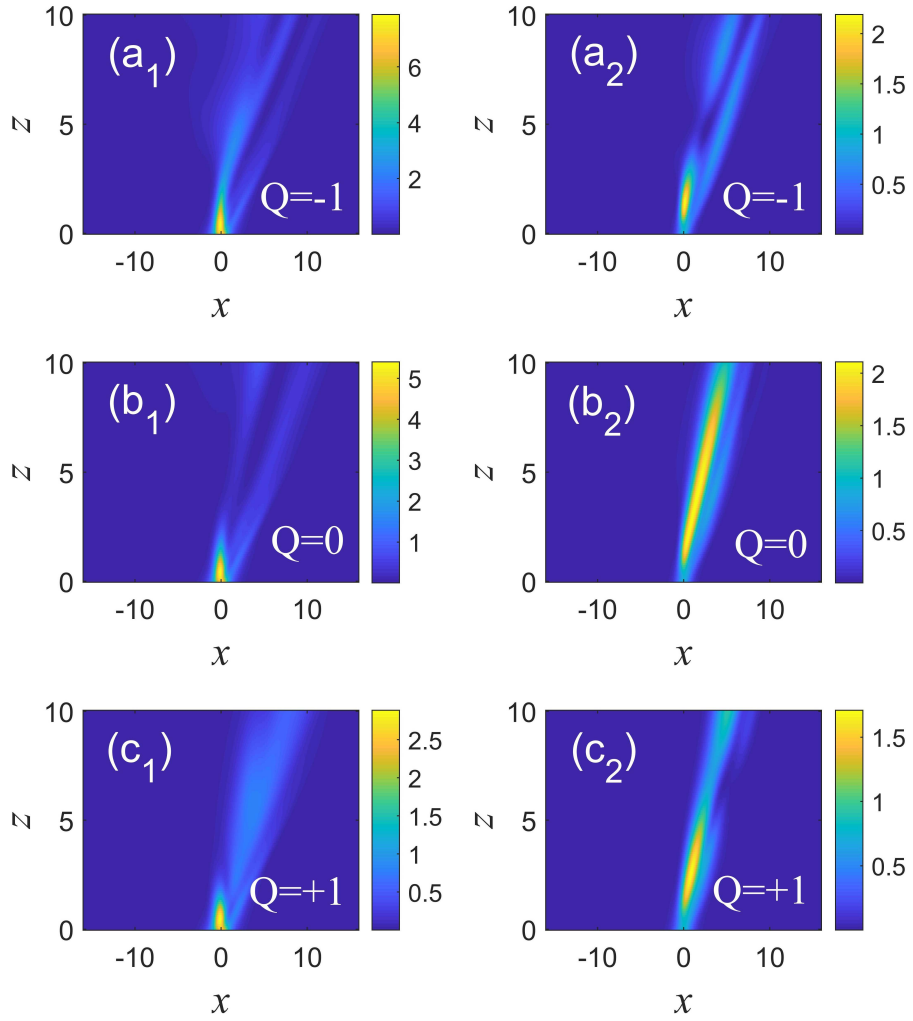


Figure 8: The same as in Fig. 7, but for  $k = 1$ . In this case, the sufficiently strong kick initiates the motion of the soliton, simultaneously destroying it.

Instead, a relatively weak kick excites robust intrinsic vibrations in the quiescent soliton, as shown in Fig. 7 for  $\alpha = 1.5$ ,  $\beta_1 = 0.5$ , and  $k = 0.3$ . It is worthy to note that the internal vibrations are very weak in the case of  $Q = -1$ , being much more conspicuous for  $Q = +1$ . This observation may be qualitatively explained by the fact that the single equation (10), to which the underlying system of Eqs. (6) and (7) is reduced by dint of the CL approximation in the case of  $Q = -1$ , is close to the usual NLS equation. Further, it is commonly known that the usual NLS bright solitons do not support any intrinsic mode, while the usual full  $\chi^{(2)}$  system, corresponding to  $Q = +1$ , gives rise to such a mode [42, 50]. While this argument helps to understand the difference between the cases of  $Q = -1$  and  $+1$  in Fig. 7, detailed studies of the intrinsic modes in solitons generated by the fractional system is a subject for a separate work, which will be reported elsewhere.

An essentially larger kick is able to set the soliton in motion, but simultaneously destroying it, as shown in Fig. 8. The possibility to create stably moving (tilted) solitons remains a subject for systematic studies. It will also be relevant to accurately identify critical values of the kick leading to the destruction of the originally quiescent solitons, and a possible link between the excitation of the above-mentioned intrinsic mode and eventual destruction.

## 5. Conclusion

We have extended the recently introduced concept of solitons in nonlinear optical waveguides with fractional diffraction for the second-harmonic-generation system with the  $\chi^{(2)}$  nonlinearity. Families of fundamental solitons have been constructed for values of Lévy index between  $\alpha = 2$ , which corresponds to the normal non-fractional diffraction, and  $\alpha = 0.5$ , which gives rise to the critical collapse, in the case of the quadratic nonlinearity, and for positive, negative, and zero values of the mismatch between the fundamental-frequency and second-harmonic components of the  $\chi^{(2)}$  system. Some characteristics of the soliton families are found in the analytical form, using the cascading limit and

scaling relations. Through the computation of stability eigenvalues for small perturbations and direct simulations of the perturbed evolution of solitons, it has been found that the Vakhitov-Kolokolov criterion for the soliton families exactly predicts their stability. In the case of  $\alpha > 0.5$ , unstable solitons spontaneously transform into robust breathers, while in the case of  $\alpha = 0.5$  the critical collapse leads to spontaneous decay of unstable solitons. The application of a relatively weak transverse kick excites small internal vibrations in the stable solitons, failing to set them in motion. A stronger kick initiates the motion (transverse tilt) of the solitons, simultaneously destroying them.

The analysis reported in this work may be developed in other directions. In particular, it may be interesting to produce fractional solitons in the two-dimensional spatial  $\chi^{(2)}$  system, as well as in the spatiotemporal one.

## 6. Acknowledgments

This work was supported by National Natural Science Foundation of China (11805141, 62205224), Guangdong Basic and Applied Basic Research Foundation (2023A1515010865), and the Scientific and Technological Innovation Programs of Higher Education Institutions in Shanxi (STIP) (2021L401). The work of D.M. was supported by the Romanian Ministry of Research, Innovation, and Digitization (PN 23210101/2023). The work of B.A.M. was supported, in part, by the Israel Science Foundation through the Grant No. 1695/22.

## Declaration of Competing Interest

The authors declare that they have no competing financial interests or personal relationships that might influence the work reported in this paper.

## References

- [1] Laskin N. Fractional quantum mechanics. *Phys Rev E* 2000;62(3):3135–45.

- [2] Laskin N. Fractional quantum mechanics and Lévy path integrals. *Phys Lett A* 2000;268(4–6):298–305.
- [3] Laskin N. Fractional Schrödinger equation. *Phys Rev E* 2002;66(5):056108.
- [4] Laskin N. Fractional quantum mechanics. World Scientific Publishing Co. Pte. Ltd.; 2018.
- [5] Stickler BA. Potential condensed-matter realization of space fractional quantum mechanics: The one-dimensional Lévy crystal. *Phys Rev E* 2013;88(1):012120.
- [6] Pinsker F, Bao W, Zhang Y, Ohadi H, Dreismann A, Baumberg JJ. Fractional quantum mechanics in polariton condensates with velocity-dependent mass. *Phys Rev B* 2015;92(19):195310.
- [7] Longhi S. Fractional Schrödinger equation in optics. *Opt Lett* 2015;40(6):1117–20.
- [8] Zhong W, Belić MR, Zhang Y. Accessible solitons of fractional dimension. *Ann Phys* 2016;368:110–6.
- [9] Zhong W, Belić MR, Malomed BA, Zhang Y, Huang T. Spatiotemporal accessible solitons in fractional dimensions. *Phys Rev E* 2016;94(1):012216.
- [10] Huang C, Dong L. Gap solitons in the nonlinear fractional Schrödinger equation with an optical lattice. *Opt Lett* 2016;41(24):5636–9.
- [11] Huang C, Dong L. Composition relation between nonlinear Bloch waves and gap solitons in periodic fractional systems. *Materials* 2018;11(7):1134.
- [12] Zeng LW, Belić MR, Mihalache D, Shi J, Li J, Li S, Lu X, Cai Y, Li J. Families of gap solitons and their complexes in media with saturable nonlinearity and fractional diffraction. *Nonlinear Dyn* 2022;108(2):1671–80.

- [13] Xiao J, Tian Z, Huang C, Dong L. Surface gap solitons in a nonlinear fractional Schrödinger equation *Opt Express* 2018;26(3):2650–8.
- [14] Huang C, Dong L. Dissipative surface solitons in a nonlinear fractional Schrödinger equation. *Opt Lett* 2019;44(22):5438–41.
- [15] Yao X, Liu X. Off-site and on-site vortex solitons in space-fractional photonic lattices. *Opt Lett* 2018;43(23):5749–52.
- [16] Zeng LW, Zeng JH. One-dimensional solitons in fractional Schrödinger equation with a spatially periodical modulated nonlinearity: nonlinear lattice. *Opt Lett* 2019;44(11):2661–4.
- [17] Chen MN, Zeng SH, Lu DQ, Hu W, Guo Q. Optical solitons, self-focusing, and wave collapse in a space-fractional Schrödinger equation with a Kerr-type nonlinearity. *Phys Rev E* 2018;98(2):022211.
- [18] Chen MN, Guo Q, Lu DQ, Hu W. Variational approach for breathers in a nonlinear fractional Schrödinger equation. *Commun Nonlinear Sci Numer Simulat* 2019;71:73–81.
- [19] Molina MI. The fractional discrete nonlinear Schrödinger equation. *Phys Lett A* 2020;384(8):126180.
- [20] Qiu YL, Malomed BA, Mihalache D, Zhu X, Zhang L, He YJ. Soliton dynamics in a fractional complex Ginzburg-Landau model. *Chaos Solitons Fractals* 2020;131:109471.
- [21] Li PF, Malomed BA, Mihalache D. Symmetry breaking of spatial Kerr solitons in fractional dimension. *Chaos Solitons Fractals* 2020;132:109602.
- [22] Wang BH, Lu PH, Dai CQ, Chen YX. Vector optical soliton and periodic solutions of a coupled fractional nonlinear Schrödinger equation. *Results Phys* 2020;17:103036.
- [23] Chen JB, Zeng JH. Spontaneous symmetry breaking in purely nonlinear fractional systems. *Chaos* 2020;30(6):063131.

- [24] Qiu YL, Malomed BA, Mihalache D, Zhu X, Peng X, He Y. Stabilization of single- and multi-peak solitons in the fractional nonlinear Schrödinger equation with a trapping potential. *Chaos Solitons Fractals* 2020;140:110222.
- [25] Li PF, Malomed BA, Mihalache D. Vortex solitons in fractional nonlinear Schrödinger equation with the cubic-quintic nonlinearity. *Chaos Solitons Fractals* 2020;137:109783.
- [26] Wang Q, Zhang LL, Malomed BA, Mihalache D, Zeng LW. Transformation of multipole and vortex solitons in the nonlocal nonlinear fractional Schrödinger equation by means of Lévy-index management. *Chaos Solitons Fractals* 2022;157:111995.
- [27] Zeng LW, Zhu YL, Malomed BA, Mihalache D, Wang Q, Long H, Cai Y, Lu XW, Li JZ. Quadratic fractional solitons. *Chaos Solitons Fractals* 2022;154:111586.
- [28] Zhong WP, Belić MR, Zhang YQ. Fractional dimensional accessible solitons in a parity-time symmetric potential. *Ann Phys* 2018;530(2):1700311.
- [29] Dong LW, Huang CM. Double-hump solitons in fractional dimensions with a  $\mathcal{PT}$ -symmetric potential. *Opt Express* 2018;26(8):10509–18.
- [30] Huang CM, Deng HY, Zhang WF, Ye FW, Dong LW. Fundamental solitons in the nonlinear fractional Schrödinger equation with a PT-symmetric potential. *Europhys Lett* 2018;122(2):24002.
- [31] Yao XK, Liu XM. Solitons in the fractional Schrödinger equation with parity-time-symmetric lattice potential. *Photonics Res* 2018;6(9):875–9.
- [32] Dong LW, Huang CM. Vortex solitons in fractional systems with partially parity-time-symmetric azimuthal potentials. *Nonlinear Dyn* 2019;98(2):1019–28.
- [33] Zhu X, Yang FW, Cao SL, Xie JQ, He YJ. Multipole gap solitons in fractional Schrödinger equation with parity-time-symmetric optical lattices. *Opt Express* 2020;28(2):1631–9.



- [34] Li PF, Malomed BA, Mihalache D. Symmetry-breaking bifurcations and ghost states in the fractional nonlinear Schrödinger equation with a PT-symmetric potential. *Opt Lett* 2021;46(13):3267–70.
- [35] Wu ZK, Yang KB, Ren XJ, Li P, Wen F, Gu YZ, Guo LJ. Conical diffraction modulation in fractional dimensions with a PT-symmetric potential. *Chaos Solitons Fractals* 2022;164:112631.
- [36] Zeng LW, Zeng JH. Fractional quantum couplers. *Chaos Solitons Fractals* 2020;140:110271.
- [37] Zeng LW, Shi JC, Lu XW, Cai Y, Zhu QF, Chen HY, Long H, Li JZ. Stable and oscillating solitons of  $\mathcal{PT}$ -symmetric couplers with gain and loss in fractional dimension. *Nonlinear Dyn* 2021;103(2):1831–40.
- [38] Zeng LW, Belić MR, Mihalache D, Wang Q, Chen JB, Shi JC, Cai Y, Lu XW, Li JZ. Solitons in spin-orbit-coupled systems with fractional spatial derivatives. *Chaos Solitons Fractals* 2021;152:111406.
- [39] Kumar S, Li PF, Malomed BA. Domain walls in fractional media. *Phys Rev E* 2022;106(5):054207.
- [40] Malomed BA. Optical solitons and vortices in fractional media: A mini-review of recent results. *Photonics* 2021;8(9):353.
- [41] Torruellas WE, Wang Z, Hagan DJ, VanStryland EW, Stegeman GI, Torner L, Menyuk CR. Observation of two-dimensional spatial solitary waves in a quadratic medium. *Phys Rev Lett* 1995;74(25):5036–9.
- [42] Pelinovsky DE, Buryak AV, Kivshar YS. Instability of solitons governed by quadratic nonlinearities. *Phys Rev Lett* 1995;75(4):591–5.
- [43] Buryak AV, Kivshar YS. Solitons due to second harmonic generation. *Phys Lett A* 1995;197(5–6):407–12.

- [44] Torner L, Mihalache D, Mazilu D, Wright EM, Torruellas WE, Stegeman GI. Stationary trapping of light beams in bulk second-order nonlinear media. *Opt Commun* 1995;121(4-6):149–55.
- [45] Mihalache D, Lederer F, Mazilu D, Crasovan LC. Multiple-humped bright solitary waves in second-order nonlinear media. *Opt Eng* 1996;35(6):1616–23.
- [46] Malomed BA, Drummond P, He H, Berntson A, Anderson D, Lisak M. Spatiotemporal solitons in multidimensional optical media with a quadratic nonlinearity. *Phys Rev E* 1997;56(4):4725–35.
- [47] Mihalache D, Mazilu D, Malomed BA, Torner L. Asymmetric spatiotemporal optical solitons in media with quadratic nonlinearity. *Opt Commun* 1998;152(4):365–70.
- [48] Yang JK, Malomed BA, Kaup DJ. Embedded solitons in second-harmonic-generating systems. *Phys Rev Lett* 1999;83(10):1958–61.
- [49] Etrich C, Lederer F, Malomed BA, Peschel T, Peschel U. Optical solitons in media with a quadratic nonlinearity. *Prog Opt* 2000;41:483–568.
- [50] Buryak AV, Trapani PD, Skryabin DV, Trillo S. Optical solitons due to quadratic nonlinearities: from basic physics to futuristic applications. *Phys Rep* 2002;370(3):63–235.
- [51] Klein MW, Enkrich C, Wegener M, Linden S. Second-harmonic generation from magnetic metamaterials. *Science* 2006;313(5786):502–4.
- [52] Sakaguchi H, Malomed BA. Vortical light bullets in second-harmonic-generating media supported by a trapping potential. *Opt Express* 2013;21(8):9813–23.
- [53] Susanto H, Malomed BA. Embedded solitons in second-harmonic-generating lattices. *Chaos Solitons Fractals* 2021;142(7):110534.

- [54] Agrawal OP. Fractional variational calculus in terms of Riesz fractional derivatives. *J Phys A: Math Theor* 2007;40(24):6287.
- [55] Cai M, Li CP. On Riesz derivative. *FCAA* 2019;22(2):287–301.
- [56] Vakhitov MG, Kolokolov AA. Stationary solutions of the wave equation in a medium with nonlinearity saturation. *Radiophys Quantum Electron* 1973;16(7):783–9.
- [57] Bergé L. Wave collapse in physics: principles and applications to light and plasma waves. *Phys Rep* 1998;303(5):259–370.
- [58] Yang JK. *Nonlinear Waves in Integrable and Nonintegrable Systems*. SIAM; 2010.